Genomics Communications

ARTICLE

Open Access

https://doi.org/10.48130/gcomm-0026-0015

Genomics Communications **2026**, 3: e016

eGPS-oneBuilder: an integrated GUI-CLI workflow for sequence-based phylogenetic tree construction, structure-informed clustering, and interactive tree interpretation

Dalang Yu[1*], Wanyu Zhang[2], Haipeng Li[2] and Lin Li[1]

[1] *School of Life Science, Hangzhou Institute for Advanced Study, University of Chinese Academy of Sciences, Hangzhou 310024, China*

[2] *Shanghai Institute of Nutrition and Health, University of Chinese Academy of Sciences, Chinese Academy of Sciences, Shanghai 200031, China*

* Correspondence: yudalang@ucas.edu.cn (Yu D)

Abstract

Phylogenetic trees are crucial for studying gene-family evolution and functional divergence. We developed eGPS-oneBuilder as an integrated, reproducible, and comparison-oriented GUI-CLI workflow for sequence alignment, trimming, multi-method tree inference, rerooting, quantitative tree comparison, and interactive visualization. The workflow connects distance, maximum-likelihood, Bayesian, and parsimony analyses, and optional protein structure-informed clustering with reusable configuration. To support interpretation across multiple trees, eGPS-oneBuilder implements two normalized summaries that quantify reference-clade recovery and branch-length variation among aligned trees. The software also provides an interactive tanglegram viewer and a pseudo-3D Tree Alignment layout for comparing more than two hierarchical structures. For proteins, Foldseek/TM-score based clustering can be used to construct structure-derived similarity trees to compensate for sequence-based phylogenetic reconstruction. We demonstrated the workflow on human *WNT-NDP* and *FZD* paralogs paired with protein structures to illuminate their phylogenetic relationship and proposed new names for *FZD* genes. Furthermore, the tree alignment analytical framework is readily extensible to single-cell sequencing analysis, enabling comparisons of cell-type clustering hierarchies across species and multi-omics contexts. We apply this extension through a real-world case study, highlighting its practical feasibility. Our results confirmed that combined sequence and structure analyses with the eGPS-oneBuilder construction, comparison, and interpretation environment can provide complementary biological insights within personal computers.

Keywords: Integrated GUI-CLI workflow, Phylogenetic tree reconstruction, Interactive visualization, Protein structure-informed tree, Interactive tanglegram, 3D Tree Alignment, Multiple tree-alignment indices

Citation: Yu D, Zhang W, Li H, Li L. 2026. eGPS-oneBuilder: an integrated GUI-CLI workflow for sequence-based phylogenetic tree construction, structure-informed clustering, and interactive tree interpretation. *Genomics Communications* 3: e016 https://doi.org/10.48130/gcomm-0026-0015

Introduction

Phylogenetic trees are widely used to study gene-family evolution, functional divergence, and molecular history[1]. Beyond serving as the end-product of an analysis, trees provide a framework for interpreting functional selection and diversification among operational taxonomic units. However, for most empirical gene-family datasets, the true evolutionary topology is unknown and independently verified gold-standard trees are rarely available[1–5]. This is especially important for gene trees, where different loci, alignment strategies, substitution models, and inference algorithms can produce alternative but biologically plausible topologies[6–9]. Phylogenetic inference is supported by several distinct methodological paradigms. Consequently, the practical challenge is not simply to infer a single tree, but to compare multiple trees, quantify their agreement and disagreement, and interactively evaluate how methodological choices influence biological interpretations. Here, sequence-based phylogenetic trees denote evolutionary reconstructions from aligned sequences, while structure-derived similarity trees denote clustering outputs based on structural similarity rather than direct phylogenetic inference.

Traditional phylogenetic workflows remain fragmented across command-line programs, file formats, visualization tools, and manually curated records. A typical analysis involves alignment and format conversion, tree inference and rerooting, visualization, and quantitative comparison. Each step introduces parameters that may influence the result. This fragmentation increases the risk of configuration errors and makes analyses harder to reproduce, audit, and communicate, particularly for non-specialist users. Existing tools address important parts of this workflow but differ in emphasis. MEGA[10] provides accessible GUI-based distance and maximum-likelihood analyses but does not provide the comparison-oriented tanglegram, multi-tree alignment, or structure-informed tree comparison environment. Geneious[11] is a broad commercial platform, yet its closed-source design limits transparent customization and reproducible replay of analytical steps. Galaxy-based pipelines[12] support reproducible web workflows but require server infrastructure and do not provide the same interactive local tree comparison views. PhyloSuite v2[13] is a recently released, freely available, integrated, and visualization-oriented phylogenetic platform with strong molecular-dating and workflow-management capabilities. However, it is oriented toward species-level multi-gene phylogenetics rather than gene-family-centric analyses and does not natively provide reproducible command-line export of GUI workflows, gene–species tree concordance quantification, or structure-informed phylogeny reconstruction.

eGPS-oneBuilder was developed to address this gap by providing an integrated, reproducible, and comparison-oriented workflow. It integrates sequence alignment, distance-based inference, maximum-likelihood inference, Bayesian inference, parsimony analysis, rerooting, pairwise tree-distance summaries, and tanglegram visualization through commonly used tools and algorithms. Rather than forcing users to select one topology prematurely, eGPS-oneBuilder

https://doi.org/10.48130/gcomm-0026-0015

makes multi-method comparison a standard part of the workflow. To support comparisons across multiple trees, it introduces tree alignment indices that summarize global tree consistency. The workflow also incorporates Foldseek-based[14] protein structure clustering, enabling comparison between sequence-derived and structure-derived hierarchies. In addition, the 3D Tree Alignment layout engine supports interactive comparison of multiple hierarchical structures, including applications to single-cell RNA-seq cell-type clustering across species and between multi-omics (RNA-seq and ATAC-seq). Overall, eGPS-oneBuilder emphasizes reproducibility, parameter transparency, quantitative comparison, and interactive interpretation on a standard personal computer.

Materials and methods

Software implementation

eGPS-oneBuilder is implemented as an integrated workflow that bridges a graphical user interface (GUI) and a command-line interface (CLI). The GUI is built on JAVA Swing and structured around seven workflow sections: Input/Align, Trim Alignment, Tree Parameters, Reroot Tree, Tree Build, Tanglegram, Visualization, and 'How to cite'. The software orchestrates MAFFT[6] for sequence alignment, PHYLIP[7] protdist/dnadist, neighbor, protpars, and dnapars for distance and parsimony analyses, IQ-TREE[8] for maximum-likelihood inference, MrBayes[9] for Bayesian inference, Foldseek[14] for protein structure comparison, and MAD[15] for midpoint ancestor divergence rerooting. Besides, TreeDist[16] and Robinson–Foulds distance[17] summaries for pairwise trees and interactive tanglegram visualization. eGPS-oneBuilder directly manages runtime configuration, PHYLIP-safe sequence-name mapping, and output organization.

Runtime parameters are stored in a JSON configuration file that enables CLI replay on Linux without manual reconstruction of method commands. The JSON records alignment settings, method enablement, IQ-TREE model strategy, model set, bootstrap replicates, optional seed and resource flags, MrBayes ngen/samplefreq/printfreq/diagnfreq and burn-in options, PHYLIP menu overrides, rerooting choices, and protein-structure options when enabled. In the default protein pipeline, IQ-TREE uses ModelFinder Plus (MFP) over the configured amino-acid model set and 1,000 ultrafast bootstrap replicates unless users override these settings in JSON. The DNA/CDS pipeline uses IQ-TREE MFP by default. MrBayes writes the executed command script and standard MrBayes output files, including sampled parameter/tree files and consensus-tree output; users should inspect the reported diagnostics, including average standard deviation of split frequencies and effective sample sizes, before interpreting the Bayesian tree. Alignment trimming is not hidden inside the tree scripts; trimmed inputs should be generated as an explicit preprocessing choice and replayed through the recorded configuration.

The runtime environment is managed via Pixi, providing a self-contained, portable execution context with apptainer (https://apptainer.org) and pixi (https://pixi.prefix.dev/latest). The root-at-midpoint, Neighbor Joining[18], or Swift Neighbor Joining algorithms are implemented in the eGPS platform[19]. See https://github.com/yudalang3/egps-oneBuilder for more information.

The eGPS-viewer is implemented totally from scratch by the power of the eGPS infrastructure.

Reproducibility and platform compatibility

For convenience, we provided the Apptainer image for a one-stop running feature. The reproducible Pixi environment can be directly run using 'git clone' or by downloading the latest zip package. We tested on Windows/WSL2, Ubuntu22.04, OS, and dependencies; example commands, input test dataset, and expected output files can be seen in the online GitHub Readme.

All pinned dependencies are specified in the pixi.toml file, (see https://github.com/yudalang3/egps-oneBuilder/blob/main/phylotree_builder_v0.0.1/pixi.toml).

Python version >= 3.12, Java version >= 25. Default parameters can be seen in https://github.com/yudalang3/egps-oneBuilder/blob/main/phylotree_builder_v0.0.1.

The eGPS-oneBuilder, which features the tree construction pipeline, is Linux-only, while the eGPS-viewer aims to be broadly portable on main operating systems. The output results of eGPS-oneBuilder can be directly imported, and other NWK tree files can also be imported into the eGPS-viewer.

Demonstration datasets

Two demonstration datasets are provided with the software. The first dataset (input_demo/prot_seqs_with_structure) contains 10 reviewed human Frizzled paralogs obtained from UniProt, paired with full-length AlphaFoldDB[12] mmCIF structural models. The second dataset (input_demo/prot_seqs_wnt_human) contains human Wnt protein sequences for sequence-only analysis. Both datasets are included in the source repository at https://github.com/yudalang3/egps-oneBuilder.

For single-cell data:

10x Genomics Multiome 3k page: www.10xgenomics.com/datasets/pbmc-from-a-healthy-donor-granulocytes-removed-through-cell-sorting-3-k-1-standard-2-0-0.

10x filtered feature-barcode H5: https://cf.10xgenomics.com/samples/cell-arc/2.0.0/pbmc_granulocyte_sorted_3k/pbmc_granulocyte_sorted_3k_filtered_feature_bc_matrix.h5.

BMC Genomics 2024 PBMC atlas article: https://bmcgenomics.biomedcentral.com/articles/10.1186/s12864-024-11030-6.

Supplementary marker workbook downloaded by the script: https://static-content.springer.com/esm/art%3A10.1186%2Fs12864-024-11030-6/MediaObjects/12864_2024_11030_MOESM5_ESM.xlsx.

Quantitative indices for tree comparison

Pairwise tree distance matrices for all generated trees were computed using the TreeDist R package[16]. This includes the classical Robinson–Foulds (RF) distance[17] to measure topological dissimilarities, and the Robinson–Foulds distance is implemented in the eGPS platform. To quantify disagreement among multiple aligned trees, we implemented pairwise distance calculations alongside two novel normalized indices introduced in eGPS-oneBuilder: the Topology Difference Index (TDI) and the Branch-Length Difference Index (BDI). In simple terms, TDI asks how often the internal clades of a chosen reference tree are recovered in the other aligned trees, whereas BDI asks how variable the corresponding branch lengths are when those clades are shared. Both indices are reference-based summaries, not symmetric all-against-all distances.

We introduced TDI and BDI to quantify topological and branch-length variation from the perspective of a fixed reference tree. To ensure reproducibility and consistency, eGPS-oneBuilder fixes the first tree in the analysis batch as the reference tree (T_1). In our default pipeline, this corresponds to the tree generated by the Distance method, or the first tree provided in the user's custom multiple-tree input. This explicit selection ensures that TDI and BDI calculations remain deterministic for a given set of inputs, addressing potential ambiguities in reference dependency. The TDI captures whether the internal clades of the reference tree are consistently

recovered across the other trees. Let N be the total number of trees. Let $C(T_1)$ be the set of all non-root internal clades in the reference tree T_1, and let $M = |C(T_1)|$ be the total number of such clades.

Each clade is uniquely identified by its clade signature (the sorted list of its descendant leaf names). For a given clade $c \in C(T_1)$, we define its recovery frequency f_c across the remaining $N - 1$ trees as:

$$f_c = \frac{1}{N-1} \sum_{i=2}^{N} I(c \in C(T_i)) \quad (1)$$

where, $I(\cdot)$ is the indicator function that equals 1 if the clade c is present in tree T_i, and 0 otherwise. The TDI is defined as the average topological difference (absence frequency) across all reference clades:

$$TDI = \frac{1}{M} \sum_{c \in C(T_1)} (1 - f_c) \quad (2)$$

TDI scales from 0 to 1, where 0 indicates that all reference clades are perfectly recovered in all other trees, and 1 indicates complete topological disagreement (no reference clades are found in any other tree).

The BDI evaluates the stability of branch lengths for the clades that are successfully recovered. It is calculated exclusively across the subset of reference clades $C^*(T_1)$ that are recovered in at least one other tree (let $M^* = |C^*(T_1)|$).

For each recovered clade $c \in C^*(T_1)$, let L_c be the set of its branch lengths from the reference tree and all the matched comparison trees. We compute the population standard deviation σ_c and the absolute mean μ_c of the branch lengths in L_c. The Coefficient of Variation (CV_c) for the clade's branch length is $CV_c = \sigma_c/\mu_c$.

To bound the variation metric between 0 and 1, we normalize the CV. The branch-length difference D_c for clade c is:

$$D_c = \frac{CV_c}{1 + CV_c} \quad (3)$$

the overall BDI is the average normalized difference across all recovered reference clades:

$$BDI = \frac{1}{M^*} \sum_{c \in C^*(T_1)} D_c \quad (4)$$

Similar to TDI, BDI is scaled from 0 (identical branch lengths across all matched clades) to approaching 1 (extreme branch-length variance). Together, TDI and BDI provide researchers with a rigorous numerical framework that complements the visual 3D tree alignment, enabling quantifiable assessments of both topological robustness and branch-length stability.

Interactive tanglegram and multiple-tree visualization

The tanglegram view was implemented for pairwise comparison of trees with matched leaf labels. It displays identical leaves across two trees, reports the Robinson–Foulds distance, and supports zooming, panning, node/branch inspection, visual-parameter adjustment, and figure export. To reduce line crossing without changing the inferred tree, eGPS-oneBuilder includes a topology-preserving leaf arrangement function. The arrangement procedure recursively sorts sister clades using three user-configurable criteria: clade size, the leaf-name string, and branch length. The default priority order is clade size, leaf-name string, and branch length, but users can reorder these criteria and choose either ascending or descending direction. This design captures common manual operations such as clade swapping and ladderization in a deterministic and reproducible form, while preserving the biological or methodological meaning of the original tree. For the multiple-tree visualization, we use Tabs to organize pairwise tanglegram views.

Pseudo-3D multiple-tree layout engine

For comparisons involving more than two trees, eGPS-oneBuilder provides a pseudo-3D alignment view. First, each input tree is converted into an internal parallelogram-level graphic tree representation. Within each tree layer, the vertical coordinate is determined by root-to-node depth, using branch lengths when available and unit depths when branch lengths are absent or non-informative. The horizontal coordinate is determined by the current leaf order after optional topology-preserving leaf arrangement. The resulting two-dimensional tree layout is then scaled to a layer-specific sheet.

The full multiple-tree scene is established by placing these sheets as parallel layers across the viewport. A fixed inter-layer spacing, oblique shear transform, floor polygon, and layer shadows are used to create a compact pseudo-3D representation. The user can reorder the displayed tree layers without changing the imported data. To highlight agreement across trees, the software identifies internal clades by their canonical descendant leaf-set signatures and can draw translucent consistency ribbons between clades or clusters that contain the identical leaf set. A quick-label mode automatically selects up to 10 internal clades from the first displayed tree and searches for their exact counterparts across the other trees, whereas manual annotation allows user-defined clade labels. The 3D view also displays the Topology Difference Index and Branch-Length Difference Index described above, providing quantitative context for the visual comparison. Rendering the 3D scene is performed in a background worker thread, and graphical updates are dispatched back to the Swing event-dispatch thread to keep the interface responsive during interactive exploration.

Simulation validation of multi-tree alignment indices

Simulation validation of multi-tree alignment indices. Balanced 16-leaf reference trees were generated with branch lengths drawn from Uniform (0.05, 0.30), providing a controlled set of internal clades for evaluating topology recovery and branch-length stability. Topological perturbation was introduced by nearest-neighbour interchange (NNI) moves, and branch-length perturbation was introduced by multiplicative Gaussian noise while preserving positive branch lengths. In addition to single-K sanity checks, we performed multi-tree calibration experiments with K = 3, 5, 10, and 20 trees. For topology calibration, the NNI perturbation fraction ranged from 0 to 1 in increments of 0.1, with 50 replicates per condition. For each simulated set, TDI and BDI were computed from the first tree as the fixed reference, matching the deterministic reference rule used by the software, whereas pairwise baselines were summarized by averaging all tree pairs within the same K-tree set. TDI was compared with mean pairwise normalized RF and mean pairwise TreeDist. Because TreeDist is not naturally bounded on the same 0–1 scale as TDI, mean pairwise TreeDist was empirically scaled to 0–1 only for calibration-error visualization. For branch-length calibration, the branch-length noise level ranged from 0 to 1 with the same K values and replication design. Runtime was benchmarked on matched K-tree inputs, excluding process startup time, to compare the practical cost of TDI/BDI calculation with pairwise TreeDist summaries. See Supplementary Material 1 for reproducible details.

Single-cell demonstration workflows

To demonstrate applications beyond conventional phylogenetics, we generated single-cell tree-alignment examples in which leaves represent annotated cell types rather than species or genes. For simulation-based demonstrations, we generated small Newick trees

https://doi.org/10.48130/gcomm-0026-0015

with matched leaf labels to mimic two common use cases: cross-species comparison of immune cell-type similarity trees and two-modality comparison between scRNA-seq and scATAC-seq. The simulated cross-species example contains human, macaque, and mouse cell-type trees with aligned immune-cell labels and is intended for the 3D multiple-tree view. The simulated multi-omics example contains paired RNA and ATAC cell-type trees with identical leaf labels and is intended for the 2D tanglegram view. These simulated files provide controlled inputs for testing import, label matching, tanglegram rendering, 3D alignment, and configuration-file handling; they are not used as evidence for biological discovery.

For the real multi-omics demonstration, we used the public 10x Genomics PBMC Multiome 3k dataset generated from paired single-cell gene-expression and chromatin-accessibility measurements (www.10xgenomics.com). Gene-expression counts were quality controlled, normalized, and summarized by marker-gene scores to assign six shared PBMC labels: CD4+ T cell, CD8+ T cell, NK cell, B cell, monocyte, and dendritic cell. RNA-based cell-type centroids were computed by aggregating normalized expression values within each assigned label. For the ATAC modality, peak accessibility from the same paired cells was converted into a marker-gene activity matrix by linking peaks to marker genes using genomic feature intervals from the 10x feature-barcode files. Peaks overlapping a gene interval expanded by 2 kb upstream and 500 bp downstream were assigned to that marker gene. Because strand information is not available in this simplified interval-based procedure, the upstream window was treated as a coordinate-neighborhood approximation rather than a promoter-direction-specific annotation. ATAC-derived marker-gene activity centroids were then computed for the same six cell-type labels. Pairwise distances among centroids were converted into hierarchical clustering trees and exported as Newick files with identical RNA and ATAC leaf labels.

For the real cross-species demonstration, Human, rhesus macaque, and mouse marker profiles were mapped to a shared set of PBMC cell-type labels and converted into species-specific cell-type similarity dendrograms[20]. The analysis used aggregated marker-profile information rather than raw cross-species single-cell matrices, which keeps the example small and reproducible while still reflecting real published immune-cell annotations. Where the source annotations did not contain a one-to-one match for a visualization label, the label was treated as a marker-based proxy. In particular, CD4+/CD8+ T-cell separation and macrophage-related labels should be interpreted as demonstration-level proxy operational taxonomic units when the original atlas annotation was broader. All single-cell outputs were written as Newick trees and accompanying oneBuilder configuration tables so that the same files can be opened directly in the 2D tanglegram and 3D multiple-tree alignment views. See Supplementary Material 2 for reproducible details.

Protein structure-informed pairwise distance calculation

A naive linear transformation from structural similarity to distance ($d = 1 - S$) fails to account for the saturation effect of structural divergence over long evolutionary timescales, which can severely compress the branch lengths of distantly related taxa and distort the inferred tree topology. To address this, we implemented a logarithmic transformation analogous to the Jukes–Cantor model of nucleotide substitution. By incorporating the empirical random baseline of TM-score ($TM_{\text{random}} = 0.17$), the structural evolutionary distance d is calculated as:

$$d = -\ln\left(\frac{S - 0.17}{1.0 - 0.17}\right) = -\ln\left(\frac{S - 0.17}{0.83}\right) \quad (5)$$

For numerical stability, the argument of the logarithm is clamped to a minimum of 10^{-6}. This produces a finite saturated maximum distance of:

$$d_{\max} = -\ln\left(10^{-6}\right) \approx 13.82 \quad (6)$$

The constants in this transformation have different interpretations. The value 0.17 is the empirical TM-score random-similarity baseline supported by the TM-score literature; 0.83 is not an independent biological parameter, but simply the normalization term 1.0–0.17, and 13.82 is not a literature-derived evolutionary coefficient, but the numerical cap implied by the 10^{-6} floor. Missing Foldseek hits are assigned this saturated distance by default, so they are treated as maximally unresolved or randomly similar pairs rather than as intermediate-distance pairs. This transformation stretches distances at the low-similarity end, but it remains a pragmatic structural-distance correction rather than a fully validated generative model of protein structural evolution. The resulting distance matrix is then used to construct a structural-derived hierarchical clustering tree using the Neighbor-Joining or SwiftNJ algorithms.

Results

A reproducible one-stop GUI-CLI bridge workflow

To overcome the major pain points in current phylogenetic pipelines (Table 1), the GUI-CLI bridge workflow is developed. The GUI system comprises two standalone yet closely integrated components: the upstream eGPS-oneBuilder module for tree construction and the downstream eGPS Tanglegram and 3D Tree Alignment Viewer, hereafter referred to as eGPS-viewer, for tree comparison and visualization. eGPS-oneBuilder is run on Linux while the eGPS-viewer is portable. eGPS-oneBuilder is structured around a guided workflow that separates input preparation, parameter editing, execution, and tanglegram inspection (Fig. 1a; Supplementary Fig. S1). The Tree Build page provides a run-focused configuration summary, live logs, method-level

Table 1. The difficulties in the current phylogenetic tree analysis pipeline and the solution of eGPS-oneBuilder.

Difficulty	eGPS-oneBuilder
No gold-standard tree for most real datasets	Generate and compare multiple plausible trees instead of reporting only one topology.
Fragmented command-line workflow	Integrate alignment, tree inference, rerooting, visualization, and comparison in one workflow, with packaged runtime support for out-of-the-box use.
Hard-to-track parameter choices	Store GUI-selected settings in a reusable runtime JSON configuration.
Limited result interpretation	Provide TreeDist/RF matrices, heatmaps, and interactive tanglegram views.
GUI and CLI are often separated	Use the GUI for setup and inspection, and the CLI for reproducible Linux execution.
Lacks intuitive graph for multiple tree alignment and quantitative metrics	Implemented an intuitive tree alignment layout engine and created the Topology Difference Index and Branch-Length Difference Index.

Fig. 1 Overview of the user-friendly oriented design of a reproducible one-stop GUI-CLI bridge workflow. (a) eGPS-oneBuilder GUI organizes input/alignment, parameter configuration, tree building, and downstream visualization in a guided tabbed workflow. The steps are organized as liner workflows, and the tab 'Tree Build' demonstrates the core step of the tree-building method with broad methodological paradigms: distance-based, parsimony, likelihood-based, and Bayesian approaches. For protein sequences, the protein structure-based clustering tree is also supported. (b) GUI-selected settings are exported as a reusable runtime JSON file and replayed by command-line scripts. The command-line interface is allowed for bioinformaticians. Users can save the configuration from the GUI and replay the analysis without intervention. Thus, the eGPS-oneBuilder implements a reproducible one-stop GUI-CLI bridge. Please see the 'Application to human WNT and FZD paralogs' section for a practical application scenario. (c) The software solves the installation pinpoint by invoking the apptainer (https://apptainer.org) and pixi (https://pixi.prefix.dev/latest) technology. The architecture of the software is structured into three layers: a top layer for user interfaces and workflow orchestration (eGPS-oneBuilder runs one), a middle layer providing essential runtimes (Java, Python, R) and analytical tools, and a bottom layer ensuring reproducible environments via Pixi and Apptainer. The dashed line means direct runs on or program dependencies, while the round rectangles represent the entities of packages. eGPS-oneBuilder is run on Linux, while the eGPS-viewer is portable and not limited to the results of eGPS-oneBuilder.

status indicators, and pre-execution validation (Fig. 1a). This design lowers the barrier for exploratory and teaching-oriented use while still exposing the method settings that influence interpretation. Parameters are organized into basic and advanced sections to support users with different levels of expertise.

The same workflow can be exported and replayed from the command line without manual intervention (Fig. 1b). This functionality is useful for manuscripts and collaborative projects because the configuration exported from the GUI also serves as a reproducible execution record. Users can therefore move from interactive desktop

https://doi.org/10.48130/gcomm-0026-0015

configuration to automated Linux execution while retaining a transparent record of inputs, methods, and parameters. For users who prefer scripted or command-line workflows, eGPS-oneBuilder can also be executed directly in CLI mode.

Protein structure-informed clustering provides complementary evolutionary information

The Protein Structure module extends the protein analysis workflow by incorporating structural similarity in addition to sequence-derived relationships (Fig. 2). With a structure mapping table, Foldseek[14] compares PDB or mmCIF structures in an all-vs-all manner and produces pairwise structural similarity scores for the starting distance-based tree. For sequence-only protein datasets, the workflow can optionally use Foldseek ProstT5/3Di representations when local ProstT5 model weights are provided by the user, ensuring explicit dependency management and avoiding unintended automatic model downloads. After the pairwise distance matrix is computed, Neighbor Joining[18] or Swift Neighbor Joining is used to construct the clustering tree.

To compare protein structures, structural similarities must be transformed into distances with care. Such transformation is not inferred under a nucleotide or amino-acid substitution model. In the eGPS-oneBuilder pipeline, the structural similarity between two proteins is quantified using the Template Modeling score (TM-score). The TM-score is a length-independent metric for assessing topological similarity, where a value of 1.0 indicates a perfect match and values below ~0.17 are generally indistinguishable from random structural similarity[21,22]. To ensure symmetry, we compute the pairwise similarity as the arithmetic mean of the query-normalized TM-score (qTM) and the target-normalized TM-score (tTM). Because protein structures are often more conserved than primary sequences[23], structure-derived clustering can reveal relationships that may be obscured in sequence-based analyses[24–26]. In this workflow (Fig. 2), structural information is treated as complementary evidence, allowing users to compare whether sequence- and structure-based trees support similar biological groupings.

Quantified indices for topological and branch-length disagreement among aligned trees

In addition to visual comparison, eGPS-oneBuilder calculates the Topology Difference Index (TDI) and Branch-Length Difference Index (BDI) to quantify disagreement among multiple aligned trees. These indices, scaled from 0 (complete agreement) toward 1 (high

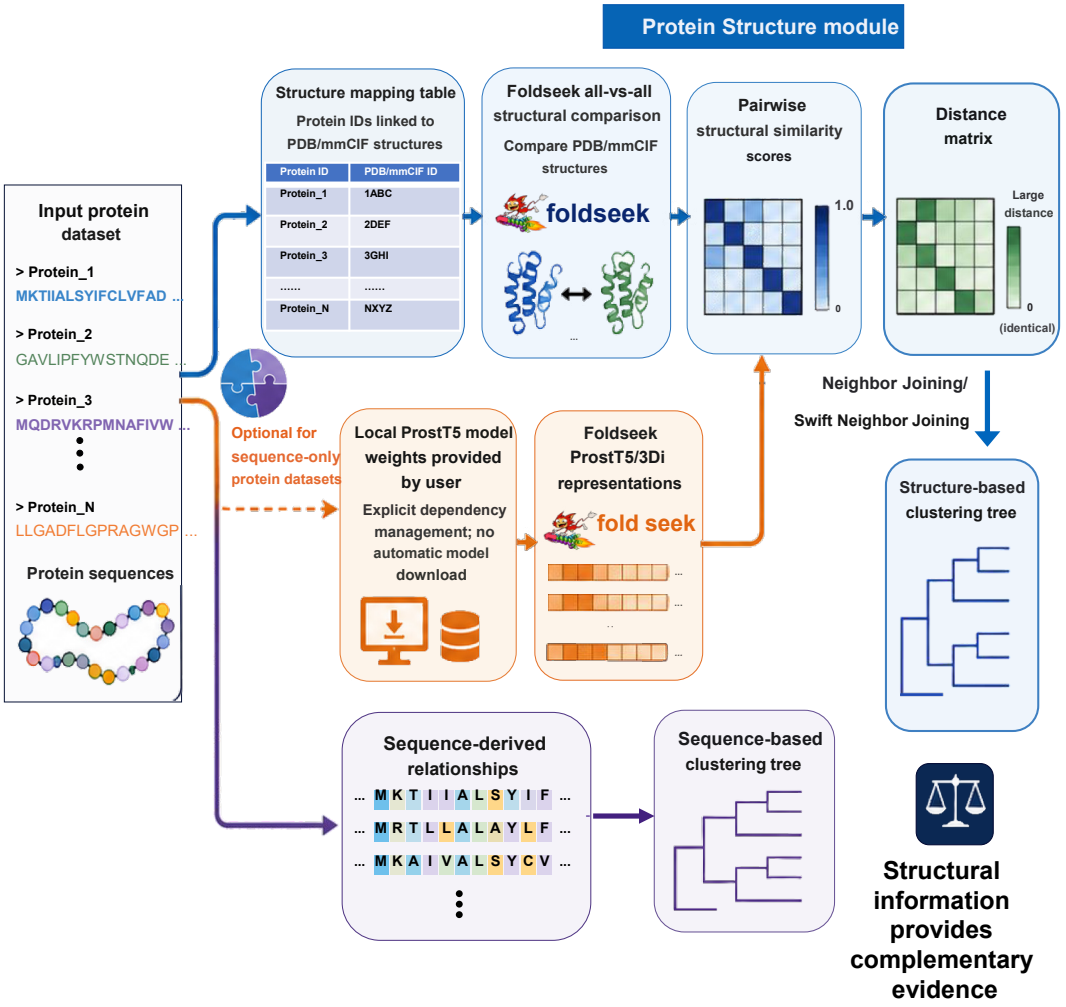

Fig. 2 Protein structure-informed hierarchical clustering analysis pipeline. Top: the Protein Structure module links protein sequences to PDB/mmCIF or AlphaFoldDB structures, performs all-vs-all structural comparison with Foldseek to produce pairwise structural similarity scores, converts structural similarity into a distance matrix, and constructs a structure-based clustering tree using NJ/SNJ algorithms. Middle: optional ProstT5/3Di representations can be used for sequence-only datasets when local model weights are supplied. Bottom: the sequence-derived relationships can be complemented by structure-informed clustering to yield biological insights.

inconsistency) nearly linearly (Fig. 3a), provide complementary summaries of tree variation: TDI captures whether the same clades are recovered across methods, whereas BDI captures how stable the corresponding branch lengths are when those clades are shared. This quantification enables researchers to move beyond visual inspection to solid numerical evaluation of topological and branch-length stability. In topology-only simulations, TDI recovered the known reference-to-other perturbation level across K = 3, 5, 10, and 20 trees (Fig. 3a), with consistently low calibration error (mean absolute error = 0.016 for all four K values). In contrast, mean pairwise normalized RF was inflated relative to the reference target (Fig. 3b), and its error increased from 0.136 at K = 3 to 0.193 at K = 20. Empirically scaled mean pairwise TreeDist showed the same pairwise-summary behavior (Fig. 3c), with higher error than TDI, increasing from 0.067 at K = 3 to 0.102 at K = 20. For all number cases, TDI shows the best minimum mean absolute error (Fig. 3d). Users are recommended to inspect the reference tree, compare TDI/BDI with pairwise RF/TreeDist matrices, and rerun the comparison with an alternative justified reference tree when conclusions are sensitive to the reference choice.

In branch-length-only simulations, BDI increased monotonically with branch-length noise (Fig. 3e), whereas mean pairwise TreeDist remained zero because topology was unchanged (Fig. 3f). The joint perturbation heatmap further showed that BDI primarily followed the branch-length noise axis among recovered clades (Fig. 3g). Finally, runtime benchmarking on the same K-tree inputs showed lower median runtime for TDI/BDI than TreeDist at K = 20 (0.609 ms vs. 43.000 ms per tree set; Fig. 3h). Together, simulation studies support the conclusion that TDI and BDI are better suited than pairwise topology-distance summaries for the specific $K > 2$ multi-tree alignment interpretation tasks addressed by eGPS-oneBuilder, while RF and TreeDist remain useful pairwise topology baselines.

Highly interactive tanglegram view and a novel multiple-tree layout engine

The tanglegram module was developed to help users visually examine differences among phylogenetic trees (Fig. 4a). After a pipeline run is completed, the viewer automatically loads the available trees, including Neighbor Joining, maximum-likelihood, Bayesian, maximum-parsimony, and, when available, the Protein Structure tree. These trees are displayed as pairwise tanglegrams, enabling users to move from numerical tree-distance results to direct visual inspection of the branches and labels that contribute to topological differences.

The feature can be used both within oneBuilder (Supplementary Fig. S2) and as a standalone viewer (Fig. 4a). In oneBuilder, the tanglegram snapshot page becomes available after a successful run and loads the current results automatically. The standalone version can open existing output folders, import custom Newick trees, and export visualizations as image files (including vector graphics) for reporting. Basic display settings, such as label size, spacing, and auto-fit options with interactive zooming in/out, moving, and querying, allow users to adjust the view for exploration or presentation.

Beyond pairwise comparison, eGPS-oneBuilder also provides a multi-tree alignment view with a novel multiple-tree layout engine in the 3D Tree Alignment (Fig. 4b). This view displays several trees together in a unified layout, allowing users to compare inferred topologies and optional structure-based clustering results in a compact and intuitive way. By presenting multiple trees side by side in an aligned visual format, the software offers a clearer and more precise overview of relationships and disagreements among different tree-building methods (see the representative case with a red arrow in Supplementary Fig. S3). The Sankey plot-style connection lines rendering is implemented to intuitively capture the consistency.

Application to human WNT and FZD paralogs

We applied the workflow to three biologically related human paralog datasets: WNT ligands, FZD receptors, and WNT-NDP, in which NDP was included as a functionally related outgroup-like protein because of its ability to activate WNT signaling. The analyses revealed clear family- and strategy-dependent differences in topological stability across 12 experimental designs and the batch GUI-CLI bridge workflow (Fig. 5a, b). FZD protein analyses had the lowest topology difference index among FZD runs (0.250) and showed strong agreement among maximum-likelihood, Bayesian, and structure-derived similarity trees (Supplementary Figs. S4, S5). In contrast, WNT was more method-sensitive: the guide-by-protein CDS regime showed the lowest WNT topology difference index (0.353), whereas trimmed CDS showed the greatest discordance (0.569) (Fig. 5c). This suggests that short, relatively divergent ligand families may benefit from protein-guided codon alignment, although this pattern is not universal; for the longer, domain-rich FZD receptors, protein-level and direct CDS signals were already comparatively stable.

The method comparison also exposed important technical behavior. Maximum parsimony frequently produced topologies that were visually and quantitatively discordant from the model-based trees, especially in WNT-NDP. By contrast, maximum likelihood and Bayesian inference consistently produced similar trees, as seen most clearly in FZD protein analyses. Neighbor joining and Bayesian inference appeared relatively stable in some comparisons, whereas likelihood topologies were more sensitive to trimming and input regime (Supplementary Material 3). These observations support the value of reporting multiple tree-building methods rather than treating one inferred topology as definitive.

Biologically, several paralog relationships were robust. In FZD, FZD3/FZD6, FZD5/FZD8, and FZD9/FZD10 recovered broadly across protein and CDS analyses, and FZD4/FZD9/FZD10 formed a stable higher-order group in model-based and structure-informed trees. FZD1, FZD2, and FZD7 did not show a single consistent branching order, although they remained structurally close. In WNT, close paralog pairs were highly conserved as terminal pairs, including WNT2/WNT2B, WNT3/WNT3A, WNT5A/WNT5B, WNT7A/WNT7B, WNT8A/WNT8B, WNT9A/WNT9B, and WNT10A/WNT10B. These pairings are consistent with recognizable duplication-derived relationships, while relationships above the pair level remained more uncertain (Supplementary Materials 3, 4 for bootstrap support values or posterior probabilities).

The WNT-NDP dataset further emphasized the distinction between protein- and CDS-level signals. Protein-based neighbor joining, maximum likelihood, Bayesian inference, and structure trees placed NDP basal to the WNT paralogs, whereas protein parsimony did not (Fig. 5d). CDS-based *NDP* placement was method-dependent, indicating that *NDP* is not reliably recognized as an outgroup-like sequence from CDS evidence alone. Thus, *NDP* provides a useful stress test for the workflow and reinforces the limited reliability of parsimony for these datasets.

These results motivate a phylogeny-informed working grouping proposal for *FZD* paralogs. WNT nomenclature already marks close paralog pairs with suffixes, such as *WNT8A*/*WNT8B* and *WNT9A*/*WNT9B*. By analogy, the stable FZD pairs could be discussed as working groups corresponding to *FZD3*/*FZD6*, *FZD5*/*FZD8*, and *FZD9*/*FZD10*. Because *FZD4* repeatedly grouped with *FZD9*/*FZD10* but was not the terminal sister of either gene, it is more cautious to describe

https://doi.org/10.48130/gcomm-0026-0015

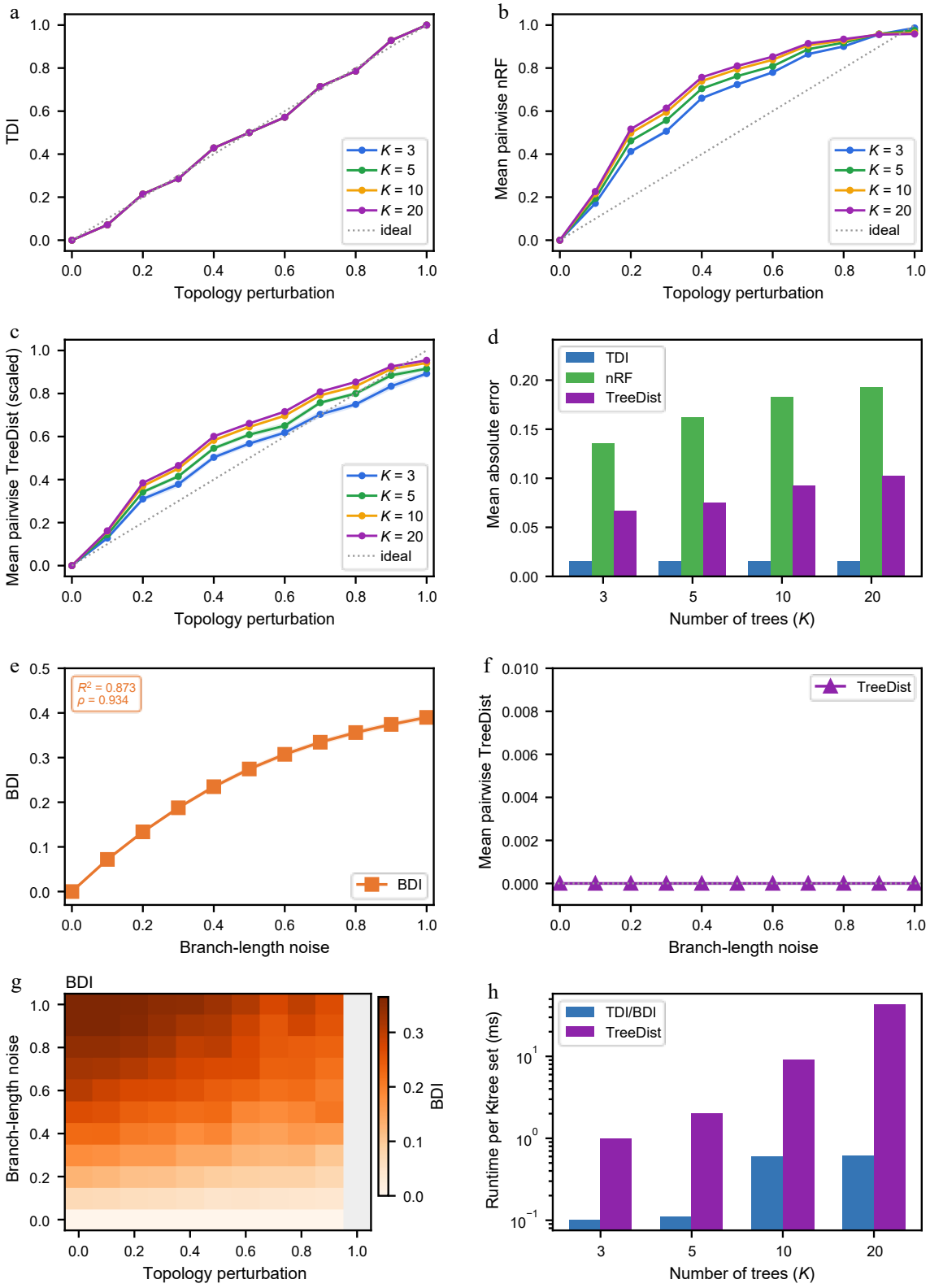

Fig. 3 Multi-tree validation of the Topology Difference Index (TDI) and Branch-Length Difference Index (BDI). (a) TDI closely recovered the known topology perturbation level across K = 3, 5, 10, and 20 aligned trees. (b) Mean pairwise normalized RF was inflated relative to the reference-to-other perturbation target because all perturbed-vs-perturbed pairs contribute to the average. (c) Mean pairwise TreeDist showed the same pairwise-summary behavior after empirical scaling to 0–1 for visual comparison. (d) Mean absolute calibration error was consistently lower for TDI than for mean pairwise normalized RF or scaled TreeDist. (e) Under branch-length-only perturbation, BDI increased with branch-length noise; R^2 denotes the linear-regression fit of BDI against the simulated noise level, and rho denotes Spearman rank correlation. (f) Mean pairwise TreeDist remained zero under the same branch-length-only perturbation because topology was unchanged. (g) The BDI heatmap uses an observation-scaled color range to emphasize vertical separation along the branch-length noise axis. (h) Runtime benchmark on the same K-tree inputs shows the median per-set runtime of TDI/BDI and TreeDist. Panels (a)–(f) and (h) used 50 replicates or benchmarked subsets from those conditions; panel (g) used 20 replicates per grid cell.

https://doi.org/10.48130/gcomm-0026-0015

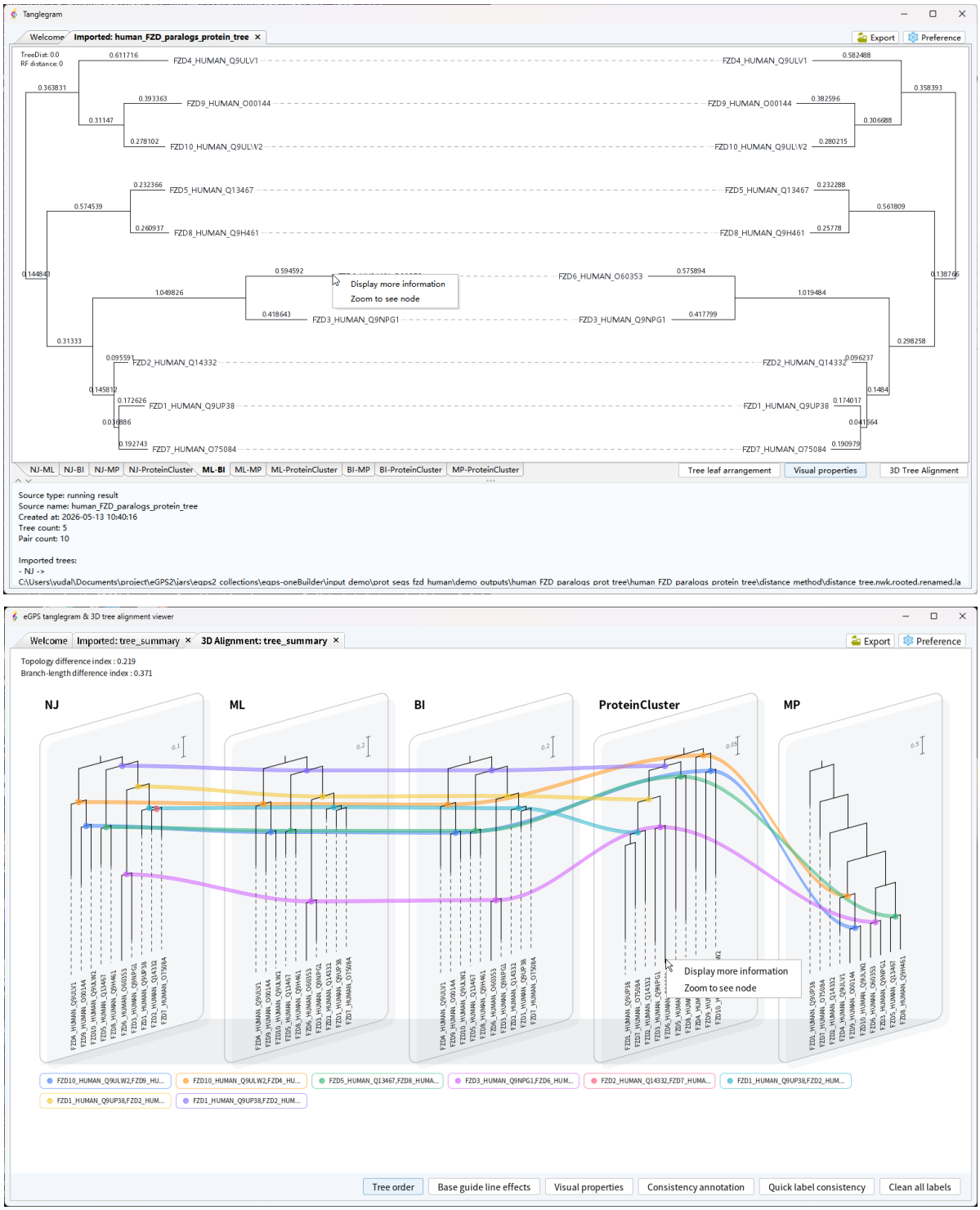

Fig. 4 A snapshot of the eGPS-viewer with a highly interactive tanglegram view and pseudo-3D Tree Alignment. (a) Standalone tanglegram viewer for pairwise tree comparison. The viewer imports eGPS-oneBuilder results or independent Newick format trees with matched leaf labels, displays selected tree pairs side by side, reports tree-distance metrics, and supports pair tabs, zooming, panning, node inspection, visual-parameter adjustment, topology-preserving leaf arrangement, and figure export. For the demonstrated six trees, a combined 10 comparison panels are displayed as tabs at the bottom. The detailed tree information is shown on the bottom console; thus, obtaining an interactive pairwise phylogenetic tree interpretation environment. (b) Pseudo-3D Tree Alignment View for multiple-tree comparison. Trees inferred by NJ, ML, BI, MP, and optional ProteinCluster methods are displayed as parallel layers. Colored consistency ribbons connect matched clades across trees, while TDI and BDI (top left) summarize topological and branch-length disagreement. The interpretation environment is organized by the Tabs on the desktop. After loading data from the Welcome page, the first visualization tab is a snapshot of the tree in a tanglegram. After clicking the '3D Tree Alignment' button, the visual demonstration appears right on the figure.

https://doi.org/10.48130/gcomm-0026-0015

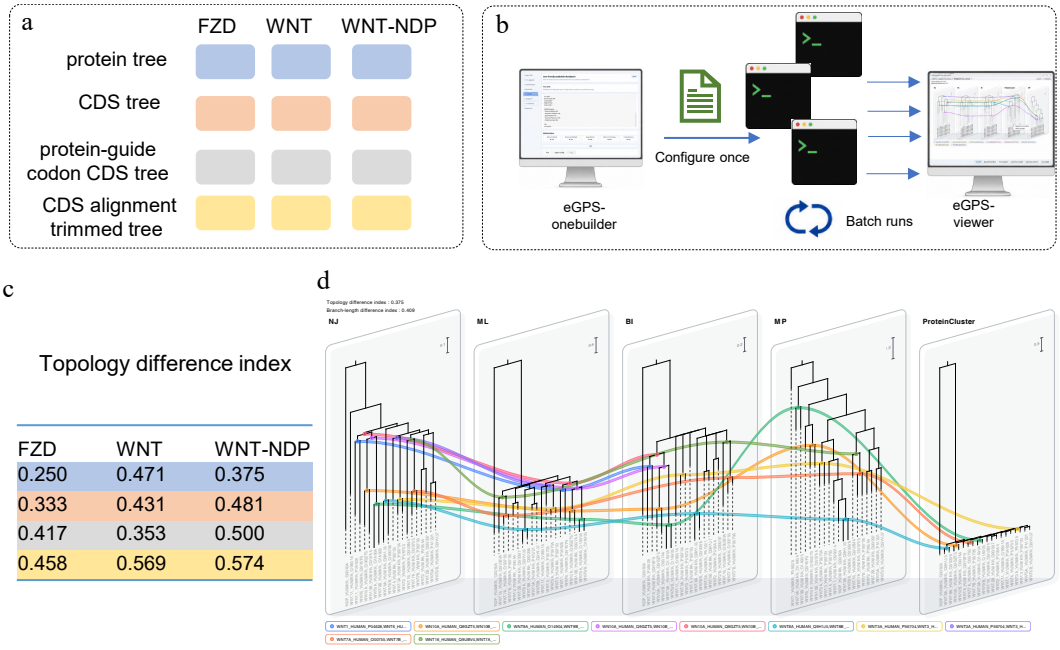

Fig. 5 Multi-method phylogenetic analysis of human WNT, FZD, and WNT-NDP paralogs. (a) Input organization and analysis design for the human FZD, WNT, and WNT-NDP datasets, each including CDS sequences, protein sequences, and corresponding predicted protein structures. Four parallel workflows were prepared for each dataset: protein-sequence tree inference with optional Foldseek-based structure clustering, untrimmed CDS tree inference after MAFFT alignment, CDS tree inference after MAFFT alignment followed by default trimming, and protein-guided CDS alignment converted from the aligned protein sequences (codon alignment). (b) eGPS-oneBuilder workflow for executing batch analyses via the GUI-CLI bridge. The workflow connects sequence alignment, optional trimming or CDS–protein alignment conversion, multi-method tree inference, quantitative topology comparison, and interactive tree visualization. Users first generate configuration files through the GUI; once generated, these configurations can be executed in batch mode, and the resulting trees can be readily inspected in the interactive visualization environment. All analyses can be performed on a standard personal computer without requiring dedicated servers, workstations, or other high-performance computing resources. (c) TDI values summarize topological disagreement across the 12 analyses. (d) 3D alignment of the WNT-NDP protein analysis shows that NDP is placed basal to WNT paralogs by NJ, ML, BI, and structure-derived similarity trees, but not by MP. See Supplementary Material 3 for details and reproducible analysis, and Supplementary Material 4 for bootstrap values and posterior probabilities.

an *FZD4-FZD9-FZD10* subgroup (See Supplementary Material 4 for bootstrap support values or posterior probabilities). *FZD1*, *FZD2*, and *FZD7* should remain unresolved in this proposal because their branching order varied across methods. Any formal gene nomenclature change would require broader taxonomic sampling, orthology/paralogy analysis, synteny, functional evidence, and consideration of existing nomenclature standards.

Proof-of-concept extending the tree alignment analytical frame to scRNA-seq analysis

The utility of tree alignment can be extended beyond conventional phylogenetic comparisons to cell-type similarity trees derived from single-cell genomics. We present this module as a proof of concept for visualizing and comparing hierarchical structures, not as a replacement for specialized single-cell integration, trajectory inference, or cell-type annotation methods. In these examples, annotated immune cell types rather than individual cells are treated as operational labels, and the resulting dendrograms are interpreted as cell-type similarity trees rather than evolutionary phylogenies. As a proof-of-concept, we generated cross-species peripheral blood mononuclear cell (PBMC) dendrograms for human, rhesus macaque, and mouse using published marker-gene profiles from a 12-species PBMC atlas[20]. Annotated immune cell types, rather than individual cells, were treated as operational taxonomic units. Because major immune cell programs are broadly conserved across vertebrates but can differ in marker expression, regulatory programs, and immune signaling across lineages[20,27], this analysis was intended to recapitulate and visualize known cross-species relationships rather than infer new evolutionary relationships. The 3D Tree Alignment module enabled direct comparison of shared immune-cell labels across species and highlighted both conserved and divergent patterns in the organization of lymphoid and myeloid cell-type groups (Fig. 6a, b). The human immune-cell tree was more similar to the rhesus tree than to the mouse tree, as reflected by the RF distances (2 in Fig. 6a vs. 4 in Supplementary Fig. S6), consistent with the expected phylogenetic relationship among these species. The global tree alignment view further revealed broadly conserved immune-cell groupings. The global alignment further revealed broadly conserved immune-cell groupings: dendritic cells, monocytes, and macrophages showed similar topology and branch-length patterns across species, and T-cell clustering was strongly conserved. In contrast, NK cells and B cells showed more divergent organization, with tangled dashed connections indicating species-specific differences in grouping patterns (Fig. 6b).

We further tested this concept using a paired single-cell multiome PBMC dataset from 10x Genomics. RNA-based annotations for six shared PBMC populations were assigned using marker-gene scores, and paired cells were aggregated by cell type to construct centroid-based dendrograms from gene expression and ATAC-derived gene-activity profiles. Gene activity was approximated by linking chromatin-accessibility peaks to marker-gene intervals using genomic coordinates from the 10x feature-barcode matrix. CD4+ and CD8+ T-cell populations clustered closely in both modalities, consistent with shared T-cell regulatory programs and RNA/ATAC

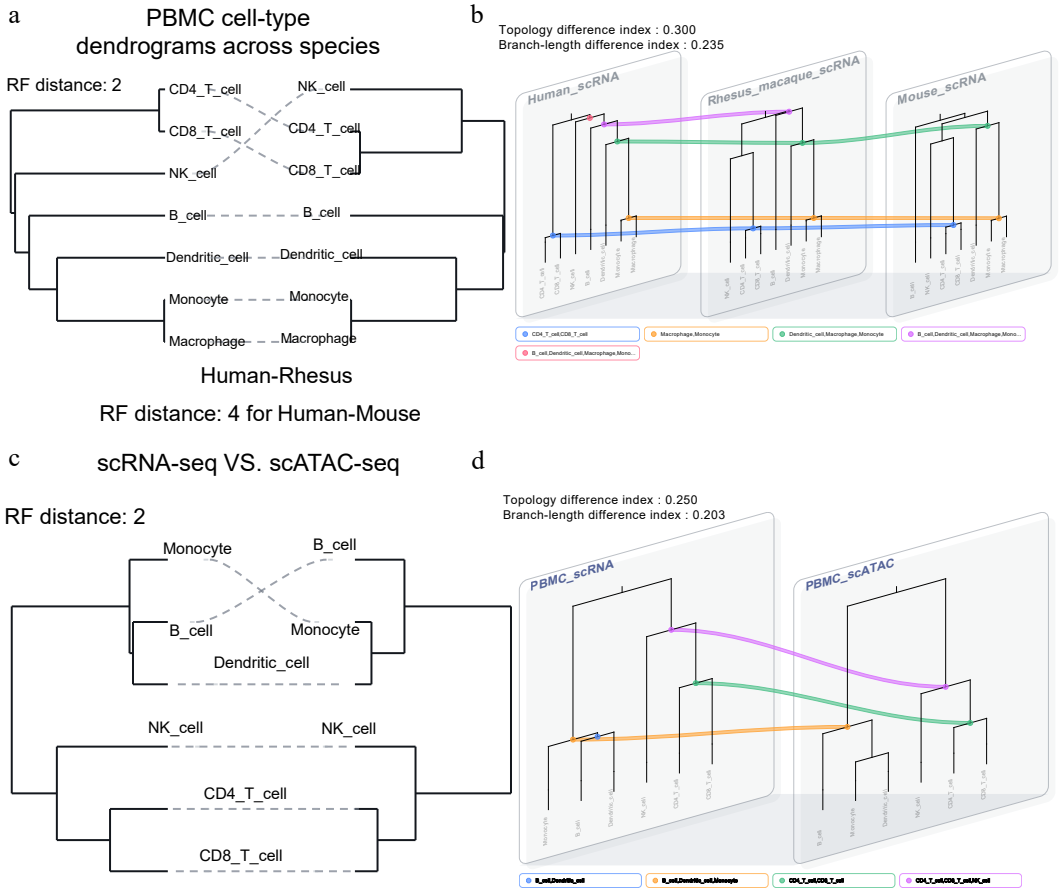

Fig. 6 Proof-of-concept extension of tree alignment to single-cell cell-type similarity dendrograms. (a) Pairwise tanglegram with Robinson–Foulds (RF) distance comparison of PBMC cell-type dendrograms among human, rhesus macaque, and mouse. The RF distance between human-rhesus is smaller than human-mouse, which is consistent with the species' evolutionary relationship. (b) 3D alignment of cross-species PBMC dendrograms highlights conserved T-cell and myeloid groupings and divergent NK/B-cell organization. (c) Pairwise tanglegram comparison of RNA- and ATAC-derived PBMC dendrograms from paired 10x multiome data. (d) Two-layer alignment of RNA and ATAC cell-type trees shows concordant CD4+/CD8+ T-cell and NK-cell relationships, with weaker agreement among other immune-cell groups.

concordance in immune multiome studies, providing a biologically expected positive control for the workflow. NK cells also showed cross-modal concordance, whereas the remaining three populations showed limited identity ambiguity (Fig. 6c, d). This example illustrates how eGPS-oneBuilder can visualize modality concordance or discordance across annotated cell populations, where aggregated cell types or clusters are more interpretable and graphically clearer.

Discussion

Phylogenetic inference is inherently uncertain, and reliance on a single topology can obscure alternative evolutionary hypotheses. eGPS-oneBuilder addresses this challenge by integrating diverse tree-building algorithms and structural comparisons into a unified workflow, allowing researchers to evaluate methodological disagreements directly rather than committing to one method *a priori* (Fig. 7). The workflow is suitable for small- to medium-scale gene-family analysis, teaching, multi-method comparison, structure/sequence tree comparison, and publication-oriented visualization.

Compared with existing tools, eGPS-oneBuilder occupies a distinct niche. MEGA[10] provides an established GUI for distance and maximum-likelihood methods. Geneious[11] offers broad functionality in a commercial package, and Galaxy-based phylogenetic pipelines[12] support web-based and server-based reproducibility. PhyloSuite[13] provides an integrated, visualization-oriented platform with advanced molecular-dating functions. eGPS-oneBuilder complements these tools by emphasizing local GUI-CLI replay, explicit multi-method tree comparison, TDI/BDI summaries, structure-informed similarity-tree comparison, and interactive tanglegram/3D Tree Alignment views for small- to medium-scale gene-family analyses and teaching-oriented workflows.

The inclusion of Foldseek-based structural comparison adds a complementary similarity perspective that is not available in conventional sequence-only pipelines. Protein structures are often more conserved than primary sequences, and structure-derived clustering trees can reveal relationships that are obscured at the sequence level. However, these trees should be interpreted as structure-informed clustering results, not as independently validated evolutionary phylogenies. Placing them alongside sequence-derived trees in the tanglegram and 3D Tree Alignment views helps users assess concordance and discordance between sequence and structural evidence.

The current implementation relies on the Pixi runtime environment on Linux for pipeline execution, while the eGPS-viewer runs on any platform with a compatible Java runtime. An Apptainer image has been provided to improve Linux deployment, and the visualization module is distributed as a plug-in on the eGPS

https://doi.org/10.48130/gcomm-0026-0015

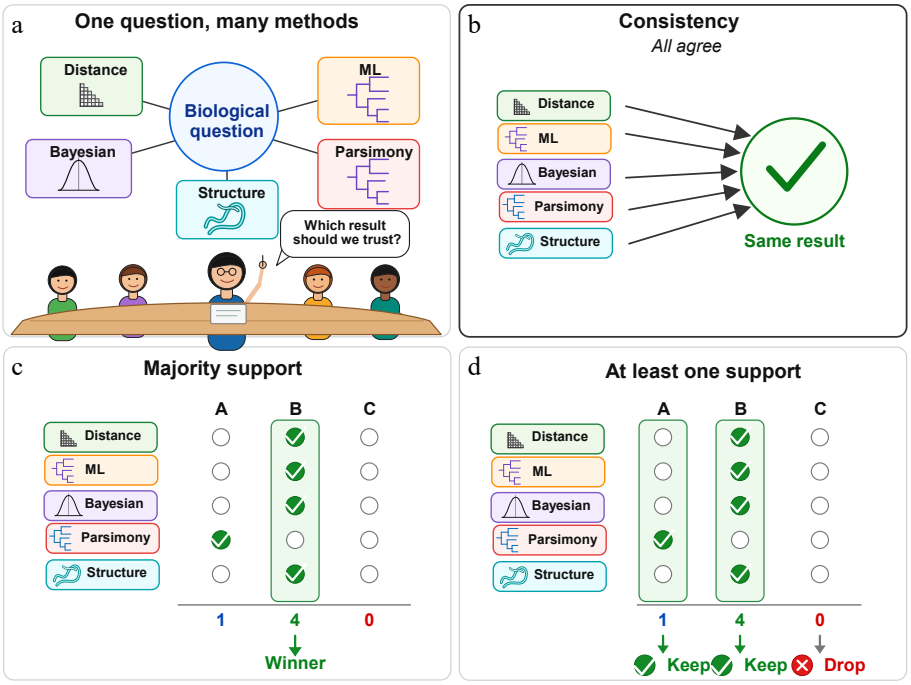

Fig. 7 Conceptual decision rules for interpreting multi-method phylogenetic results in eGPS-oneBuilder. (a) A single biological question can be evaluated by multiple complementary approaches, including distance-based inference, maximum likelihood (ML), Bayesian inference, parsimony, and protein structure-informed clustering. The central challenge is deciding which inferred relationship should be trusted or retained. (b) Under a strict consistency rule, a result is accepted only when all methods support the same conclusion. (c) Under majority support, the candidate supported by most methods is selected as the primary result. (d) Under an at-least-one-support rule, any candidate supported by one or more methods is retained for further interpretation, whereas unsupported candidates are discarded. This framework emphasizes that multi-method phylogenetic analysis should not force premature selection of a single topology, but should make agreement, disagreement, and alternative biologically plausible hypotheses explicit.

platform[19]. Several limitations should be noted. The demonstration datasets are limited in taxonomic breadth, structure-derived similarity trees are not substitutes for formal evolutionary models, and TDI/BDI depend on the chosen reference tree. Performance on very large alignments has not been systematically benchmarked; analyses involving thousands of sequences or extensive bootstrap/MCMC settings may require command-line execution, additional memory, and future HPC workflow integration.

Conclusions

We present eGPS-oneBuilder, a comprehensive GUI-CLI workflow that streamlines phylogenetic analysis by integrating sequence alignment, multi-method tree inference, quantitative topology comparison, and interactive visualization within a reproducible framework. The software introduces a pseudo-3D Tree Alignment visualization engine and two interpretable indices, TDI and BDI, for assessing tree agreement. By incorporating protein structure-based clustering via Foldseek, eGPS-oneBuilder provides complementary evolutionary evidence that can reveal relationships obscured in sequence-based analyses. Beyond phylogenetics, the tree alignment framework is readily extensible to other hierarchical datasets, including scRNA-seq cell-type clustering, highlighting its broader applicability in computational biology. eGPS-oneBuilder is freely available at https://github.com/yudalang3/egps-oneBuilder.

Ethical statements

During the preparation of this work, the author used ChatGPT and Gemini for language refinement. The author reviewed and edited all content produced with the assistance of this tool, verified its accuracy, and took full responsibility for the integrity andoriginality of the final manuscript. This work represents the author's own intellectual contribution, and no AI tool is credited as an author.

Author contributions

The authors confirm their contributions to the paper as follows: data curation, formal analysis, investigation, methodology, software, writing – original draft: Yu D, Zhang W; conceptualization, supervision: Yu D, Li L; validation, visualization: Yu D, Li L, Li H; funding acquisition, project administration, resources: Yu D; writing – review and editing: Yu D, Zhang W, Li H, Li L. All authors reviewed the results and approved the final version of the manuscript.

Data availability

The source code and demonstration datasets are freely available at https://github.com/yudalang3/egps-oneBuilder.

Acknowledgments

This work was supported by the Youth Fund of the National Natural Science Foundation of China (No. 32400511) to DY.

Conflict of interest

The authors declare that they have no conflict of interest.

Supplementary information accompanies this paper online at: https://doi.org/10.48130/gcomm-0026-0015.

Dates

Received 24 May 2026; Revised 15 June 2026; Accepted 24 June 2026; Published online 20 July 2026

References

[1] Kapli P, Yang Z, Telford MJ. 2020. Phylogenetic tree building in the genomic age. *Nature Reviews Genetics* 21:428–444

[2] Degnan JH, Rosenberg NA. 2006. Discordance of species trees with their most likely gene trees. *PLoS Genetics* 2:e68

[3] Degnan JH, Rosenberg NA. 2009. Gene tree discordance, phylogenetic inference and the multispecies coalescent. *Trends in Ecology & Evolution* 24:332–340

[4] Hanson-Smith V, Kolaczkowski B, Thornton JW. 2010. Robustness of ancestral sequence reconstruction to phylogenetic uncertainty. *Molecular Biology and Evolution* 27:1988–1999

[5] Salichos L, Rokas A. 2013. Inferring ancient divergences requires genes with strong phylogenetic signals. *Nature* 497:327–331

[6] Katoh K, Standley DM. 2013. MAFFT multiple sequence alignment software version 7: improvements in performance and usability. *Molecular Biology and Evolution* 30:772–780

[7] Felsenstein J. 1985. Confidence limits on phylogenies: an approach using the bootstrap. *Evolution* 39:783–791

[8] Wong TKF, Ly-Trong N, Ren H, Demotte P, Baños H, et al. 2026. IQ-TREE 3: phylogenomic inference software using complex evolutionary models. *Molecular Biology and Evolution* 43:msag117

[9] Ronquist F, Teslenko M, van der Mark P, Ayres DL, Darling A, et al. 2012. MrBayes 3.2: efficient Bayesian phylogenetic inference and model choice across a large model space. *Systematic Biology* 61:539–542

[10] Stecher G, Suleski M, Tao Q, Tamura K, Kumar S. 2026. MEGA 12.1: cross-platform release for macOS and linux operating systems. *Journal of Molecular Evolution* 94:14–18

[11] Kearse M, Moir R, Wilson A, Stones-Havas S, Cheung M, et al. 2012. Geneious Basic: an integrated and extendable desktop software platform for the organization and analysis of sequence data. *Bioinformatics* 28:1647–1649

[12] Community TG, Abueg LAL, Afgan E, Allart O, Awan AH, et al. 2024. The Galaxy platform for accessible, reproducible, and collaborative data analyses: 2024 update. *Nucleic Acids Research* 52:W83–W94

[13] Zhao D, Ye T, Gao F, Jakovlić I, La Q, et al. 2025. PhyloSuite v2: the development of an all-in-one, efficient and visualization-oriented suite for molecular dating analysis and other advanced features. *iMeta* 4:e70095

[14] van Kempen M, Kim SS, Tumescheit C, Mirdita M, Lee J, et al. 2024. Fast and accurate protein structure search with Foldseek. *Nature Biotechnology* 42:243–246

[15] Tria FDK, Landan G, Dagan T. 2017. Phylogenetic rooting using minimal ancestor deviation. *Nature Ecology & Evolution* 1:193

[16] Smith MR. 2020. Information theoretic generalized Robinson-Foulds metrics for comparing phylogenetic trees. *Bioinformatics* 36:5007–5013

[17] Llabrés M, Rosselló F, Valiente G. 2021. The generalized Robinson-foulds distance for phylogenetic trees. *Journal of Computational Biology* 28:1181–1195

[18] Saitou N, Nei M. 1987. The neighbor-joining method: a new method for reconstructing phylogenetic trees. *Molecular Biology and Evolution* 4:406–425

[19] Yu D, Dong L, Yan F, Mu H, Tang B, et al. 2019. eGPS 1.0: comprehensive software for multi-omic and evolutionary analyses. *National Science Review* 6:867–869

[20] Zhang S, Fang X, Chang M, Zheng M, Guo L, et al. 2024. Cross-species single-cell analysis reveals divergence and conservation of peripheral blood mononuclear cells. *BMC Genomics* 25:1169

[21] Xu J, Zhang Y. 2010. How significant is a protein structure similarity with TM-score = 0.5? *Bioinformatics* 26:889–895

[22] Zhang C, Shine M, Pyle AM, Zhang Y. 2022. US-align: universal structure alignments of proteins, nucleic acids, and macromolecular complexes. *Nature Methods* 19:1109–1115

[23] Illergård K, Ardell DH, Elofsson A. 2009. Structure is three to ten times more conserved than sequence—a study of structural response in protein cores. *Proteins: Structure, Function, and Bioinformatics* 77:499–508

[24] Chothia C, Lesk AM. 1986. The relation between the divergence of sequence and structure in proteins. *The EMBO Journal* 5:823–826

[25] Zhang S, Zhang T, Fu Y. 2023. Proteome-wide structural analysis quantifies structural conservation across distant species. *Genome Research* 33:1975–1993

[26] Puente-Lelievre C, Malik A, Douglas J. 2025. Protein structural phylogenetics. *Genome Biology and Evolution* 17:evaf139

[27] Jiao A, Zhang C, Wang X, Sun L, Liu H, et al. 2024. Single-cell sequencing reveals the evolution of immune molecules across multiple vertebrate species. *Journal of Advanced Research* 55:73–87